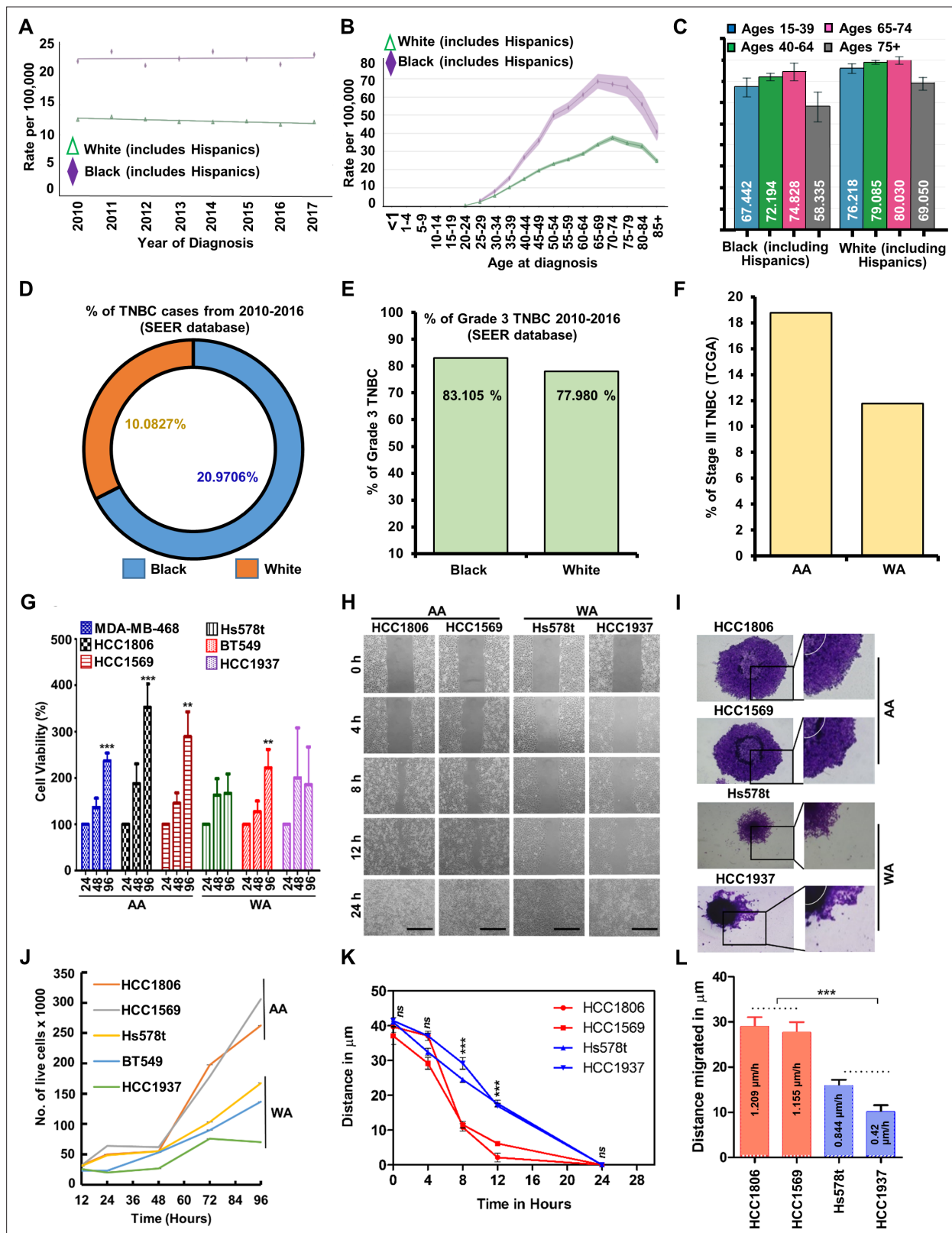


---

## Figures and figure supplements

Concomitant activation of GLI1 and Notch1 contributes to racial disparity of human triple negative breast cancer progression

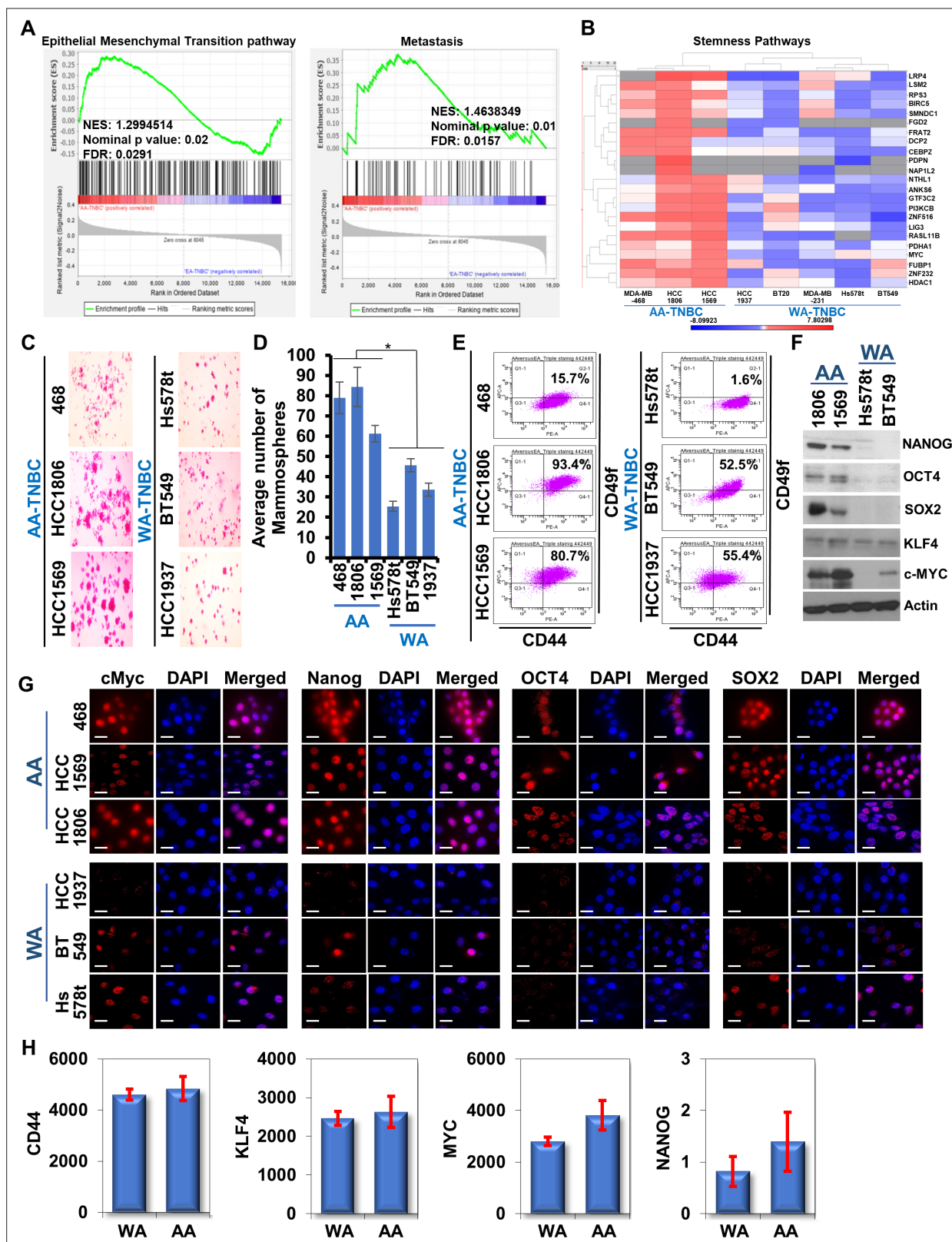
**Sumit Siddharth *et al***



**Figure 1.** African American (AA) women exhibit higher triple negative breast cancer (TNBC) incidence and related mortality and AA-TNBC cells possess higher proliferation and migration potential compared to White American (WA) women. (A) Race-specific incidence rate of TNBC (female only) (Surveillance, Epidemiology, and End Results [SEER] data). (B) Age-wise incidence of TNBC per 100,000 black (including Hispanics) vs. white (including Hispanics) women. (C) Five-year relative survival rates of TNBC (female only) in black (including Hispanics) vs. white women (including Hispanics). (D) Figure 1 continued on next page

*Figure 1 continued*

Percentage of TNBC cases in AA vs. WA women (SEER data). **(E)** Percentage of Grade 3 tumors in AA and WA women (SEER data). **(F)** Percentage of Stage III TNBC among AA vs. WA women from the TCGA dataset. **(G)** Bar graph shows % cell viability of MDA-MB-468, HCC1806, HCC1569, Hs578t, BT549, and HCC1937 cells. **(H, K)** Representative images of HCC1806, HCC1569, Hs578t, and HCC1937 cells undergoing scratch migration assay. Images are captured at different time intervals as indicated. Graph shows a quantitative representation of distance remaining in the original scratch (width) as cells migrate over time. Scale bar 40  $\mu\text{m}$ . **(I, L)** Spheroid migration of HCC1806, HCC1569, Hs578t, and HCC1937 cells. Representative images of spheroids are shown. Graph shows average distance migrated. Data represents  $n = 3$  independent experiments.  $*p \leq 0.05$ ,  $**p \leq 0.01$ ,  $***p \leq 0.001$  **(J)** HCC1806, HCC1569, Hs578t, BT549, and HCC1937 cells were grown for 12, 24, 36, 48, 60, 72, 84, and 96 hr, and then subjected to trypan blue dye exclusion assay.



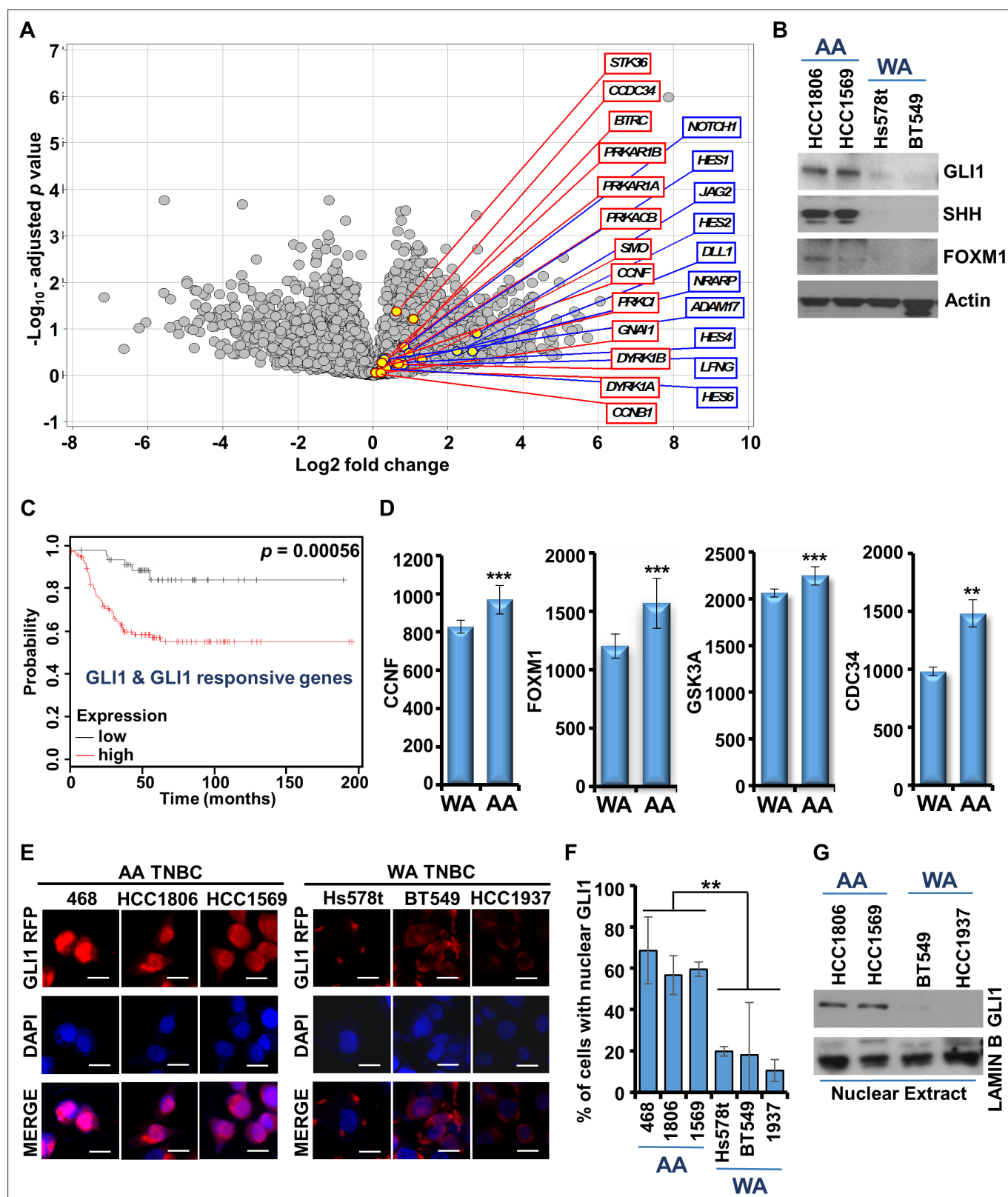
**Figure 2.** African American (AA)-triple negative breast cancer (TNBC) cells possess higher stem cell enriched population than White American (WA)-TNBC cells. (A) Gene set enrichment analysis (GSEA) of hallmark epithelial-mesenchymal transition and Tavazoie metastasis pathway in cancer between AA-TNBC samples and WA-TNBC samples from GSE46581 dataset (Gene Expression Omnibus). (B) Differential expression statistics comparing AA-TNBC cells (MDA-MB-468, HCC1806, HCC1569) with WA-TNBC cells (Hs578t, BT549, BT20, HCC1937, MDA-MB-231) were calculated and results are

Figure 2 continued on next page



*Figure 2 continued*

shown in a heatmap ( $p \leq 0.05$ ). Genes are marked on the side. **(C, D)** Representative images of mammospheres formed by HCC1806, HCC1569, MDA-MB-468, HCC1937, BT549, and Hs578t cells. Bar graphs show quantification of solid mammospheres. Data represents  $n = 4$  independent experiments.  $*p \leq 0.05$ . **(E)** Flow cytometry analysis of AA-TNBC and WA-TNBC cells using CD44 and CD49f staining. **(F)** Immunoblot analysis of NANOG, OCT4, SOX2, KLF4, and c-MYC in HCC1806, HCC1569, Hs578t, and BT549 cells. Expression of ACTB served as the loading control. **(G)** Immunofluorescence analysis of cMyc, OCT4, NANOG, and SOX2 in MDA-MB-468, HCC1569, HCC1806, HCC1937, BT549, and Hs578t cells. Nuclei are stained with DAPI. Scale bar, 20  $\mu\text{m}$ . **(H)** Normalized mRNA expression of CD44 ( $*p = 0.102$ ), KLF4 ( $*p = 0.010$ ), MYC ( $*p = 0.002$ ), and NANOG ( $*p = 0.023$ ) in WA- and AA-TNBC patients from TCGA and Affymatrix datasets.

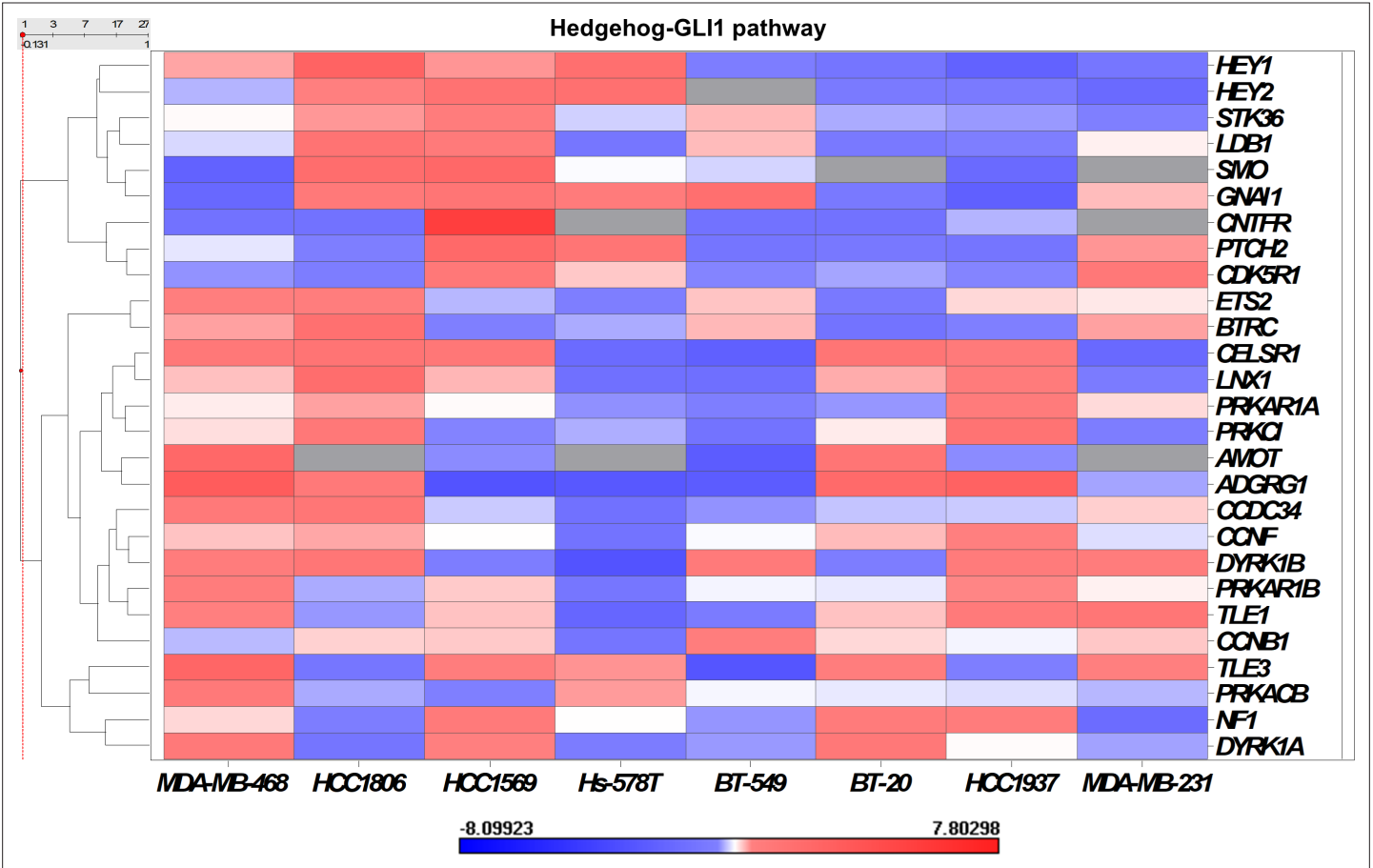


**Figure 3.** GLI1 and Notch1 pathways are upregulated in African American (AA)-triple negative breast cancer (TNBC) in comparison to White American (WA)-TNBC. **(A)** Differential expression statistics comparing AA-TNBC cells with WA-TNBC cells were calculated and results are shown in a volcano plot. Upregulation of GLI1-responsive genes (marked in red) and Notch1 responsive genes (marked in blue) as observed in gene expression analyses is shown. **(B)** Immunoblot analysis of GLI1, SHH, and FOXM1 in HCC1806, HCC1569, Hs578t, and BT549 cells. Expression of actin serves as the loading

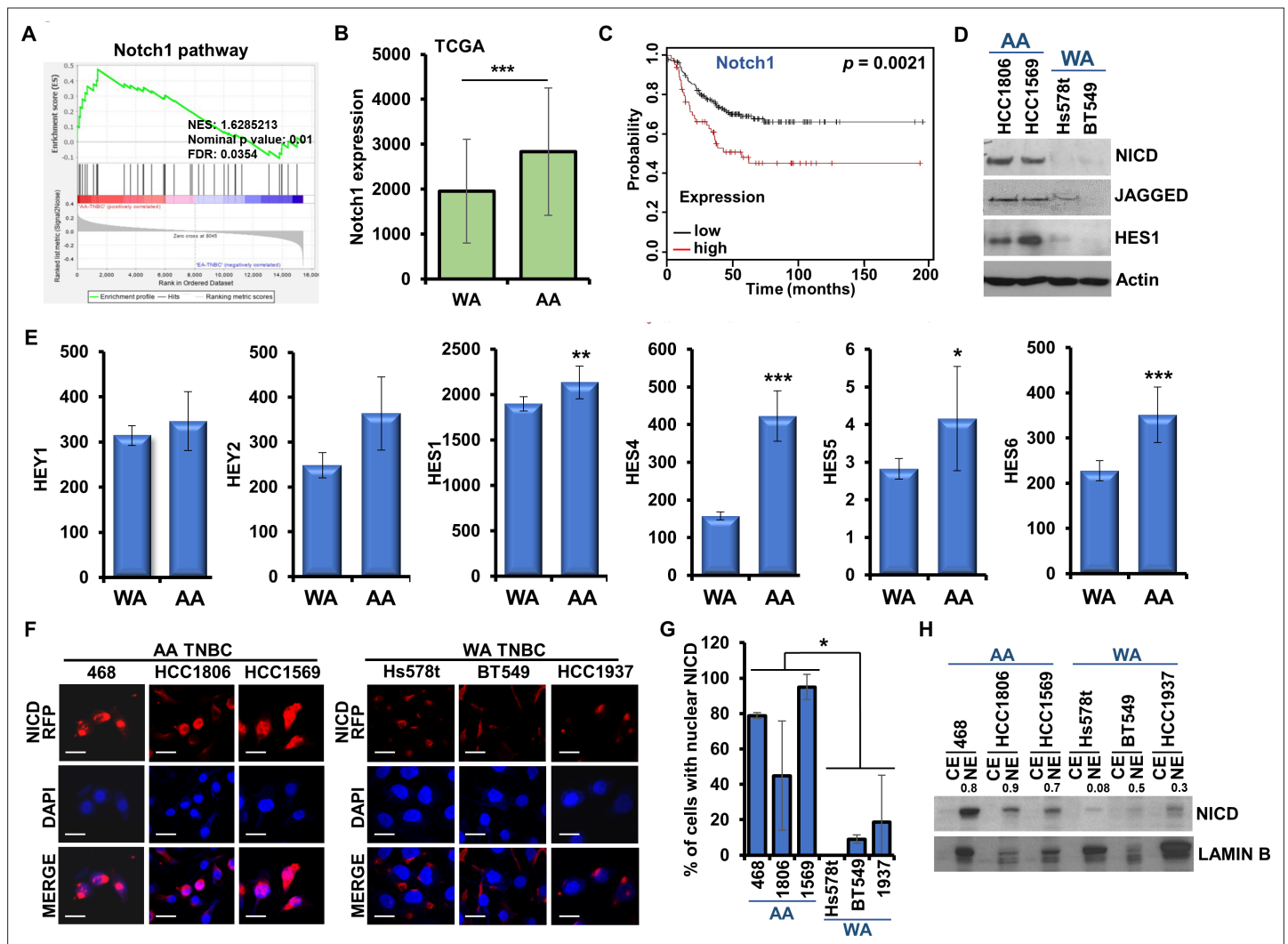
Figure 3 continued on next page

*Figure 3 continued*

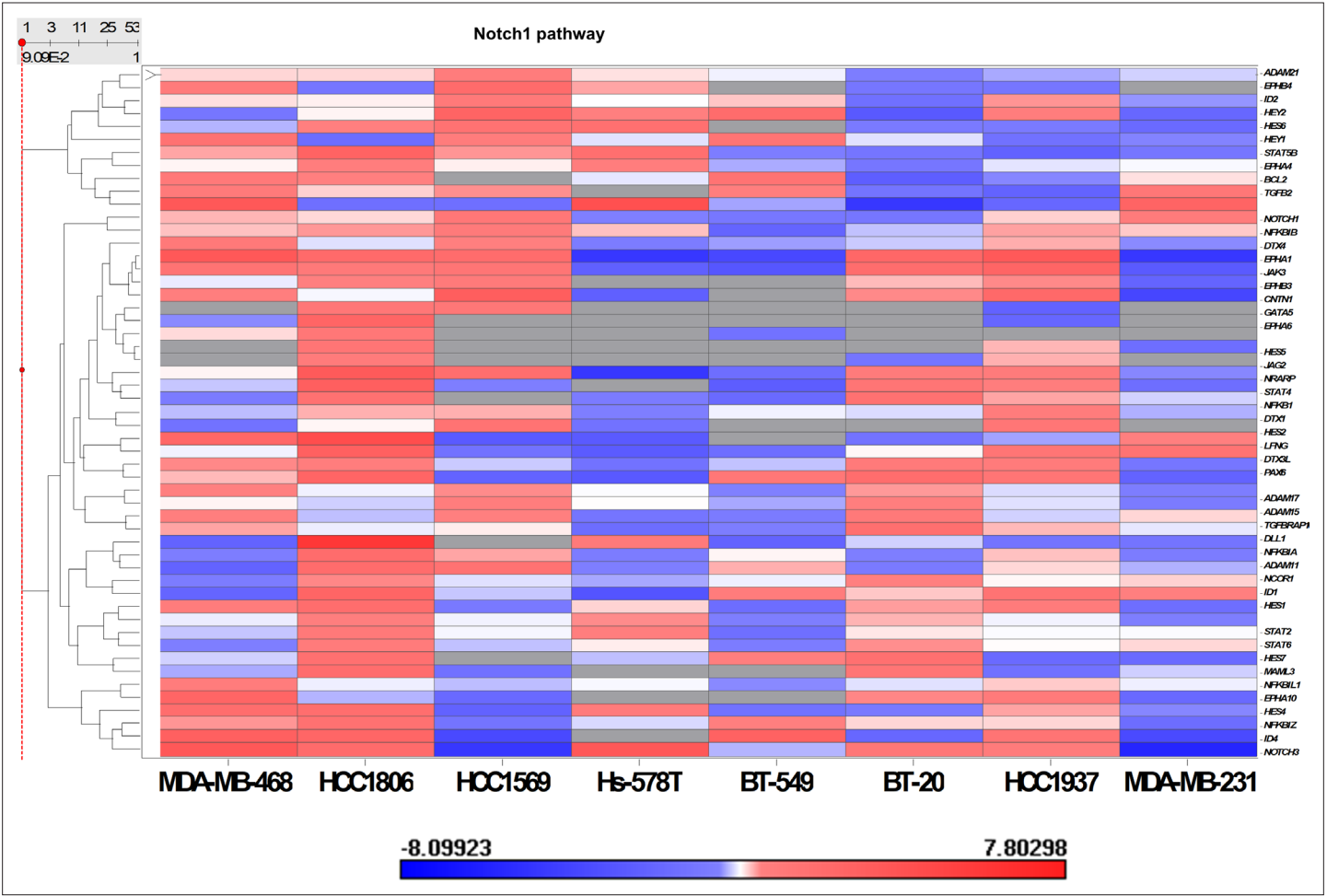
control. **(C)** Kaplan–Meier curve showing recurrence-free survival (RFS) for the TNBC patients with high or low GLI1 and GLI1 target gene expression. \* $p = 0.00056$ . **(D)** Normalized mRNA expression of GLI1 target genes in WA-TNBC and AA-TNBC patients, respectively, from TCGA cohort. \*\* $p \leq 0.01$ , \*\*\* $p \leq 0.001$ . **(E, F)** Immunofluorescence analysis of GLI1 in MDA-MB-468, HCC1806, HCC1569, Hs578t, BT549, and HCC1937 cells. Bar graphs show quantitation of cells with nuclear GLI1 expression. Data represents  $n = 4$  independent experiments. \*\* $p \leq 0.01$ . Scale bar, 20  $\mu\text{m}$ . **(G)** Immunoblot analysis of GLI1 in the nuclear extracts in HCC1806, HCC1569, BT549, and HCC1937 cells. Lamin B is used as control.



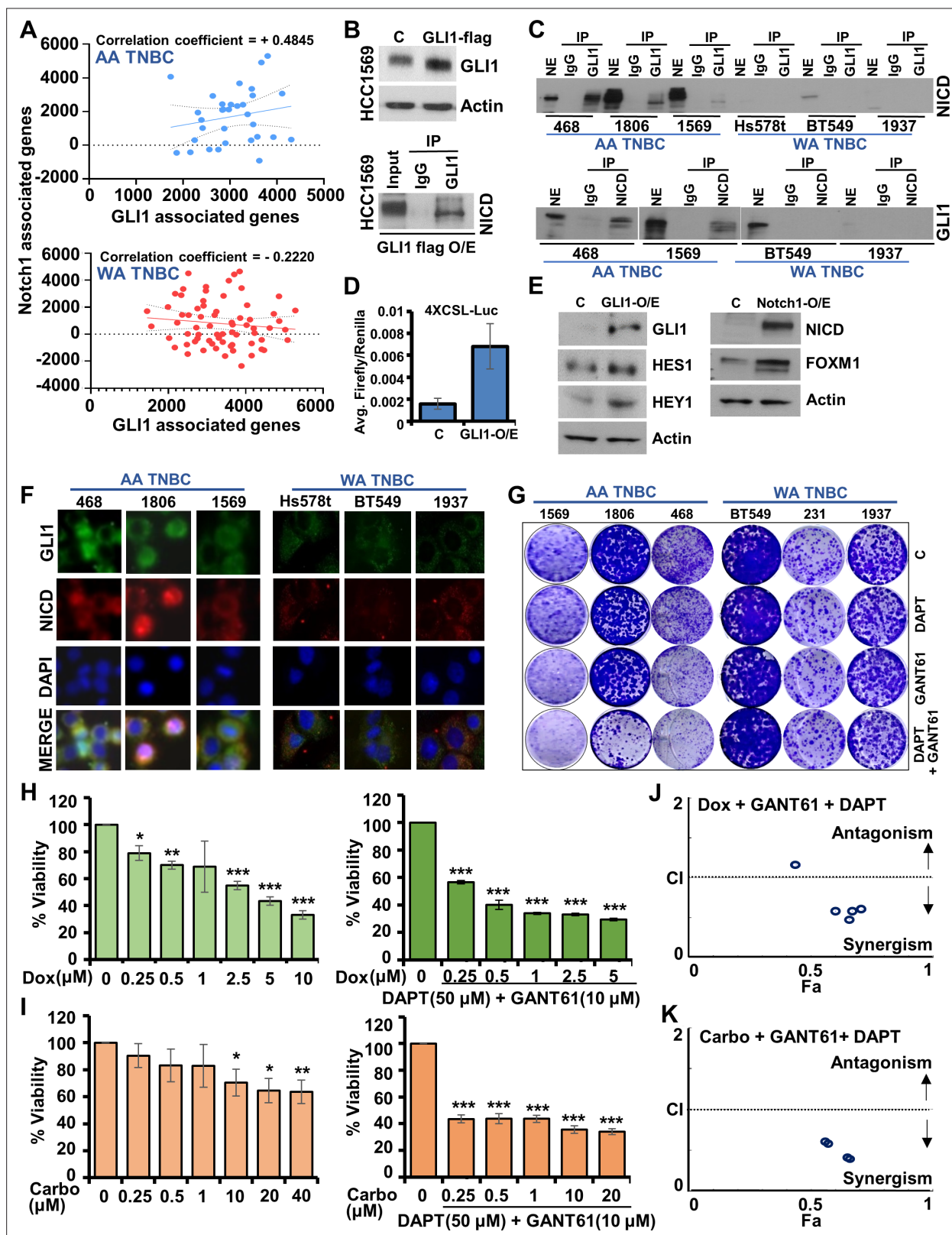
**Figure 3—figure supplement 1.** Increased expression of GLI1 pathway genes in African American (AA)-triple negative breast cancer (TNBC) cell lines compared to White American (WA)-TNBC cell lines. Differential expression statistics comparing AA-TNBC cells (MDA-MB-468, HCC1806, HCC1569) with WA-TNBC cells (Hs578t, BT549, BT20, HCC1937, MDA-MB-231) were calculated and results are shown in a heatmap. Genes are marked on the side.



**Figure 4.** African American (AA)-triple negative breast cancer (TNBC) cells exhibit increased activation of Notch1, a key protein associated with poor survival. **(A)** Gene set enrichment analysis (GSEA) of Notch1 pathway between AA-TNBC samples and White American (WA)-TNBC samples from GSE46581 dataset (Gene Expression Omnibus). **(B)** Normalized average Notch1 mRNA expression in AA (n = 32) and WA (n = 68) TNBC patients, respectively, from TCGA cohort. (\*\*p < 0.01). **(C)** Kaplan-Meier curve showing recurrence-free survival (RFS) for the TNBC patients with high and low Notch1 expression. p = 0.0021. **(D)** Immunoblot analysis of Notch intracellular domain (NICD), JAGGED, and HES1 in HCC1806, HCC1569, Hs578t, and BT549. Actin serves as the loading control. **(E)** Normalized mRNA expression of Notch1 target genes (HEY/HES family genes) in WA- and AA-TNBC patients, respectively, from TCGA cohort. (\*p < 0.05, \*\*p < 0.01, \*\*\*p < 0.001). **(F, G)** Immunofluorescence analysis of NICD in MDA-MB-468, HCC1806, HCC1569, Hs578t, BT549, and HCC1937 cells. Bar graphs show quantitation of cells with nuclear NICD expression. Data represents n = 4 independent experiments. \*p < 0.05. Scale bar, 20  $\mu$ m. **(H)** Immunoblot analysis of NICD in the nuclear extracts in MDA-MB-468, HCC1806, HCC1569, BT549, and HCC1937 cells. Lamin B is used as control.



**Figure 4—figure supplement 1.** Upregulated expression of Notch1 pathway genes in African American (AA)-triple negative breast cancer (TNBC) cell lines compared to White American (WA)-TNBC cell lines. Differential expression statistics comparing AA-TNBC cells (MDA-MB-468, HCC1806, HCC1569) with WA-TNBC cells (Hs578t, BT549, BT20, HCC1937, MDA-MB-231) were calculated and results are shown in a heatmap. Genes are marked on the side.



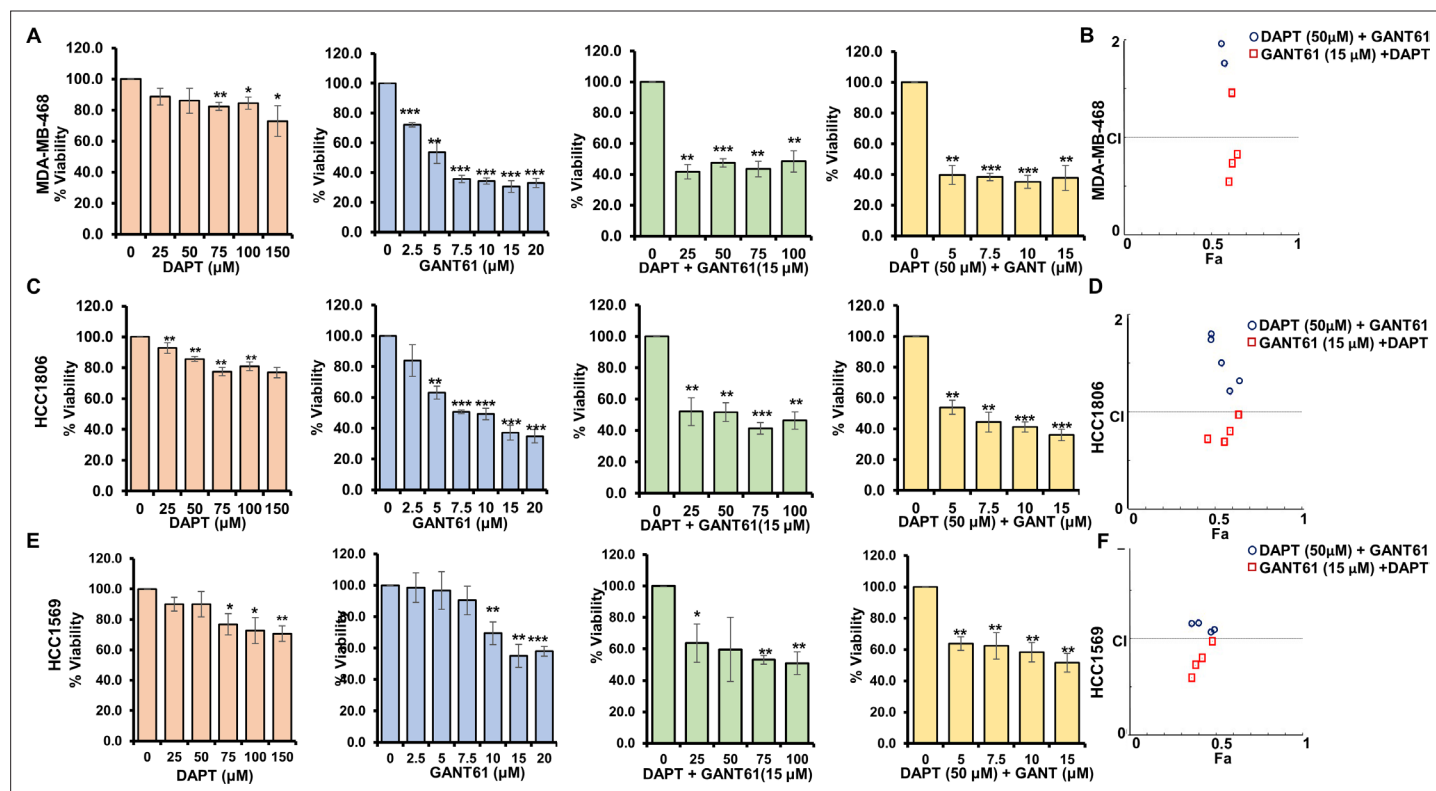
**Figure 5.** Concomitant upregulation, co-localization, and interaction of GLI1 and Notch intracellular domain (NICD) in African American (AA)-triple negative breast cancer (TNBC). (A) Co-expression of GLI1 gene signature and Notch1 gene signature in AA-TNBC (n = 32, R = +0.4845) and White American (WA)-TNBC from TCGA cohort (n = 68, R = -0.2220). (B) Immunoblot analysis of GLI1 and actin in the nuclear extract of HCC1569 cells transfected with Flag-GLI1 overexpression constructs. Immunoprecipitation of GLI1 from the nuclear extracts of cells transfected with Flag-GLI1

Figure 5 continued on next page



## Figure 5 continued

overexpression constructs and immunoblotting with NICD antibodies. **(C)** Co-immunoprecipitation of NICD with GLI1 from the nuclear extracts of MDA-MB-468, HCC1806, HCC1569, Hs578t, BT549, and HCC1937 cells. Lower panel shows co-immunoprecipitation of GLI1 with NICD from the nuclear extracts of MDA-MB-468, HCC1569, BT549, and HCC1937 cells. NE (nuclear extract input), IP (immunoprecipitation). **(D)** Luciferase activity of 4XCSL-Luc in MDA-MB-468 cells transfected with GLI1 overexpression construct. **(E)** HCC1806 cells were transfected with Flag-GLI1 overexpression construct and lysates were immunoblotted for Notch-responsive genes – Hey1 and Hes1. HCC1806 cells were transfected with Notch1 overexpression construct and lysates were immunoblotted for GLI1-responsive gene – FOXM1. Actin serves as the loading control. **(F)** Immunofluorescence analysis of NICD and GLI1 in MDA-MB-468, HCC1806, HCC1569, Hs578t, BT549, and HCC1937 cells. Nuclei are stained with DAPI. Scale bar, 20  $\mu$ m. **(G)** Representative images of colonies formed by AA-TNBC and WA-TNBC cells treated with DAPT (50  $\mu$ M), GANT61 (10  $\mu$ M), and the combination of DAPT (50  $\mu$ M) and GANT61 (10  $\mu$ M) in a clonogenicity assay. **(H, I)** Cell viability assay of HCC1806 cells treated with doxorubicin, carboplatin, doxorubicin + DAPT (50  $\mu$ M) + GANT61 (10  $\mu$ M) and carboplatin + DAPT (50  $\mu$ M) + GANT61 (10  $\mu$ M) as indicated for 24 hr. \* $p \leq 0.05$ , \*\* $p \leq 0.01$ , \*\*\* $p \leq 0.001$ . **(J, K)** Synergistic interaction between the fixed concentration of DAPT (50  $\mu$ M) + GANT61 (10  $\mu$ M) treatment with a varied concentration of doxorubicin (0.25, 0.5, 1, 2.5, and 5  $\mu$ M) and carboplatin (0.25, 0.5, 1, 10, and 20  $\mu$ M), respectively.



**Figure 5—figure supplement 1.** Synergistic effect of GLI1 and Notch1 inhibitors in reducing the viability of African American (AA)-triple negative breast cancer (TNBC) cells. **(A, C, E)** 3-(4,5-Dimethylthiazol-2-yl)-2,5-diphenyltetrazolium bromide (MTT) cell viability assay of **(A)** MDA-MB-468, **(C)** HCC1806, and **(E)** HCC1569 cells treated with the indicated concentrations ( $\mu\text{M}$ ) of DAPT (peach bar graph), GANT61 (blue bar graph), GANT61 (15  $\mu\text{M}$ ) + DAPT (25, 50, 75, 100  $\mu\text{M}$ , respectively) (green bar graph) and DAPT (50  $\mu\text{M}$ ) + GANT61 (5, 7.5, 10, 15  $\mu\text{M}$ , respectively) (yellow bar graph) for 24 hr ( $*p \leq 0.05$ ,  $**p \leq 0.01$ ,  $***p \leq 0.001$ ). **(B, D, F)** Synergistic interaction between DAPT and GANT61 represented from CI value calculated using the Chou-Talalay method. CI < 1, CI = 1, CI > 1 indicates synergistic, additive, and antagonistic effects, respectively.

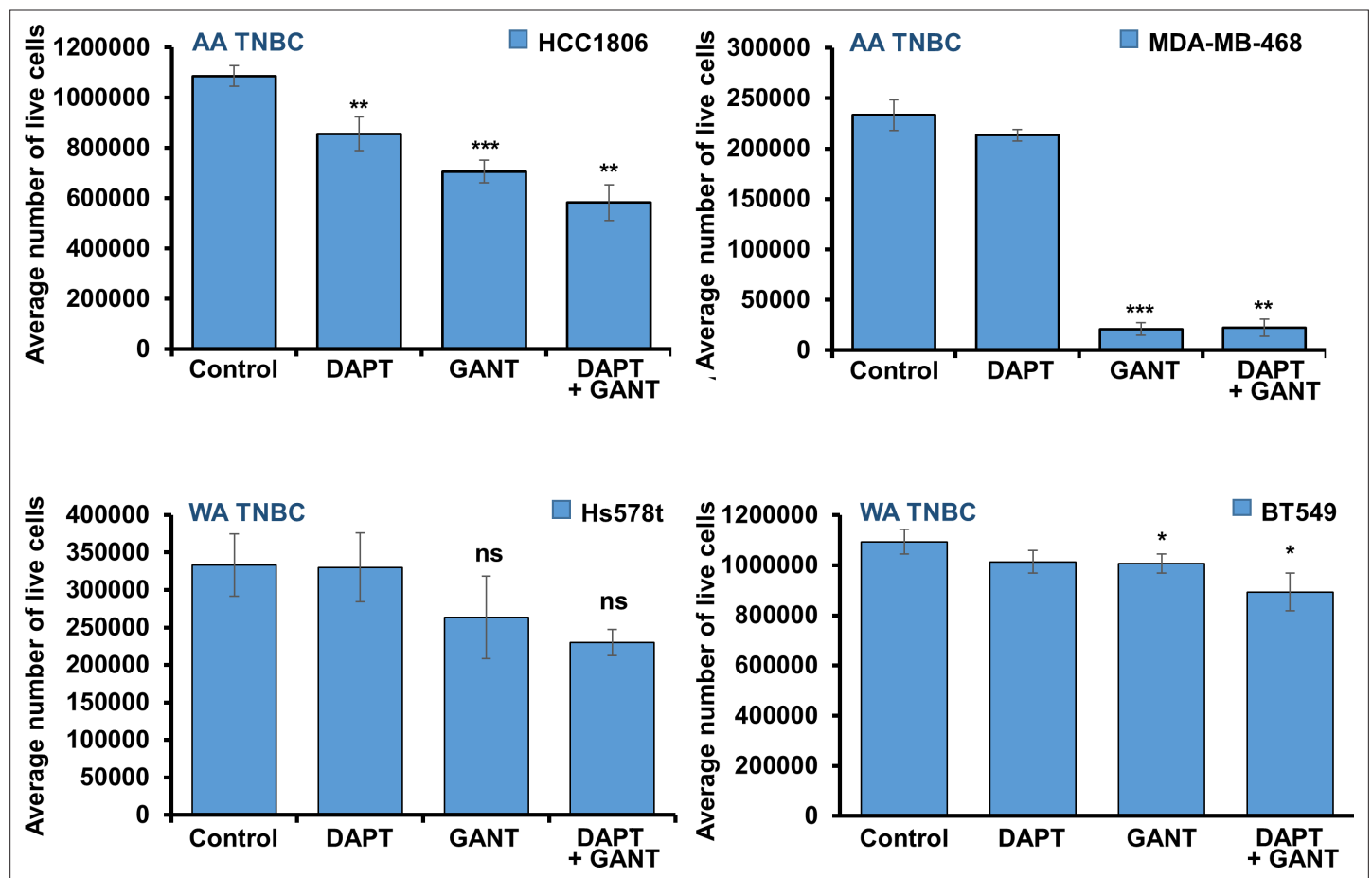


**Figure 5—figure supplement 2.** Effect of GLI1 and Notch1 inhibitors on the viability of African American (AA)-triple negative breast cancer (TNBC) and White American (WA)-TNBC cells. HCC1806, MDA-MB-468, Hs578t, and BT549 cells were treated with DAPT (50  $\mu$ M) and/or GANT61 (15  $\mu$ M) alone or in combination as indicated. Bar graph shows % cell viability of cells. (\*p ≤ 0.05, \*\*p ≤ 0.01, \*\*\*p ≤ 0.001).

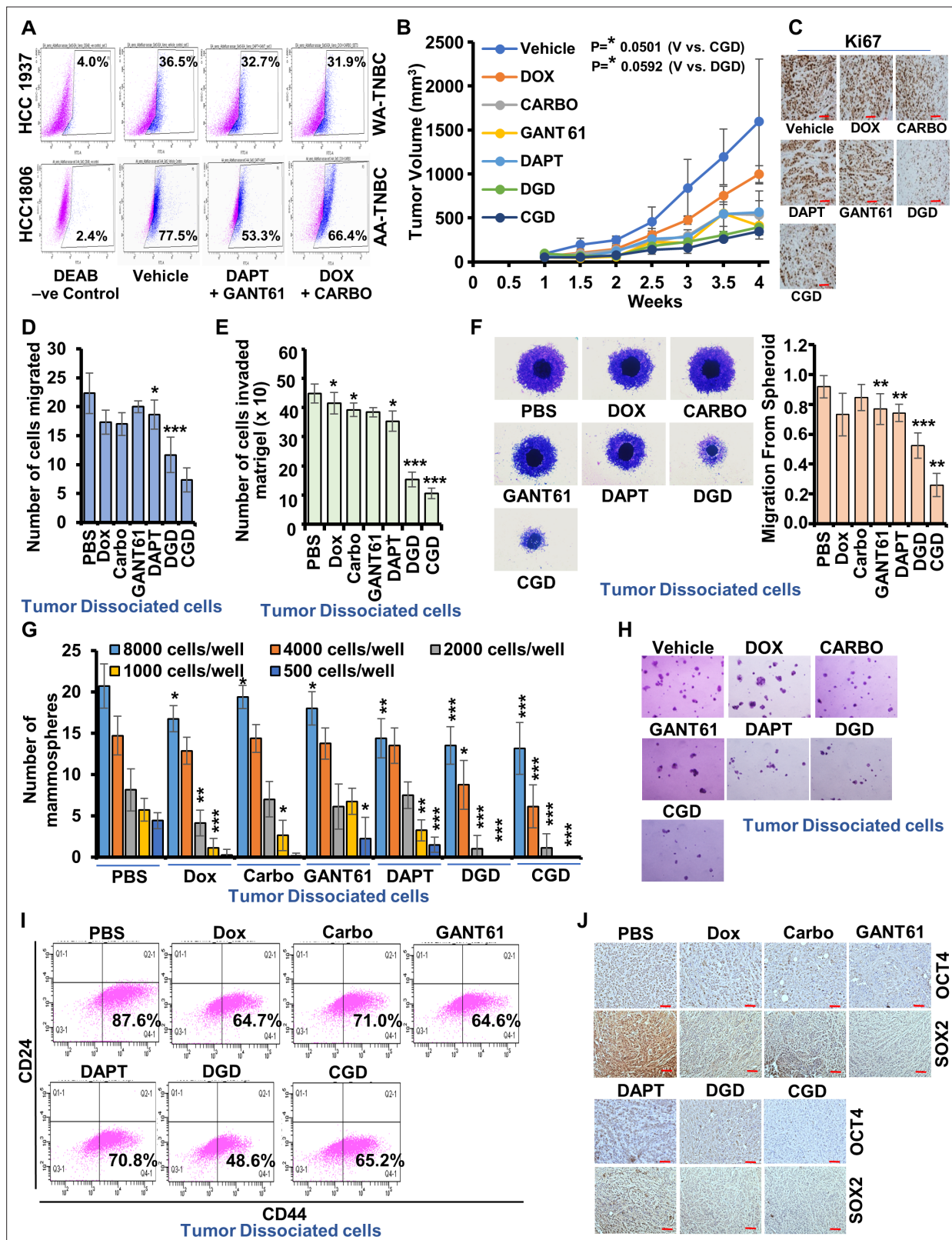
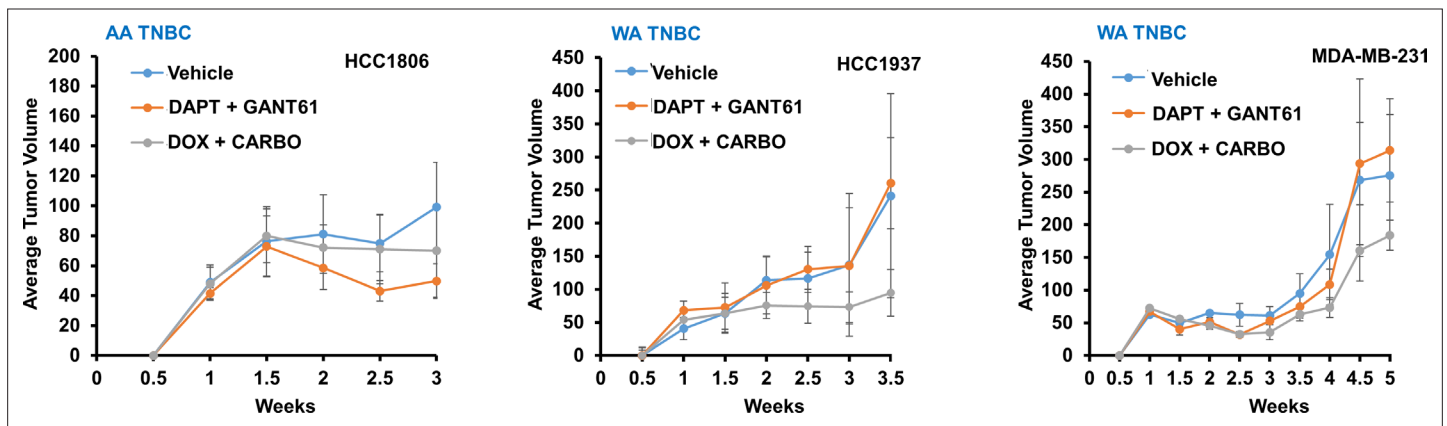


**Figure 6.** Combined treatment with chemotherapy, Notch inhibitor, and GLI1 inhibitor blocks African American (AA)-triple negative breast cancer (TNBC) tumor progression. (A) ALDH activity assay for dissociated tumor cells from HCC1937 and HCC1806 tumors treated with DAPT + GANT61 and doxorubicin + carboplatin combination. (B) Line graph shows tumor progression curves of HCC1806-derived tumors (n = 6) treated with vehicle, doxorubicin, carboplatin, GANT61, DAPT, DAPT + GANT61 + doxorubicin and CARBO + GANT61 + DAPTplatin. (C) Representative images of Ki67

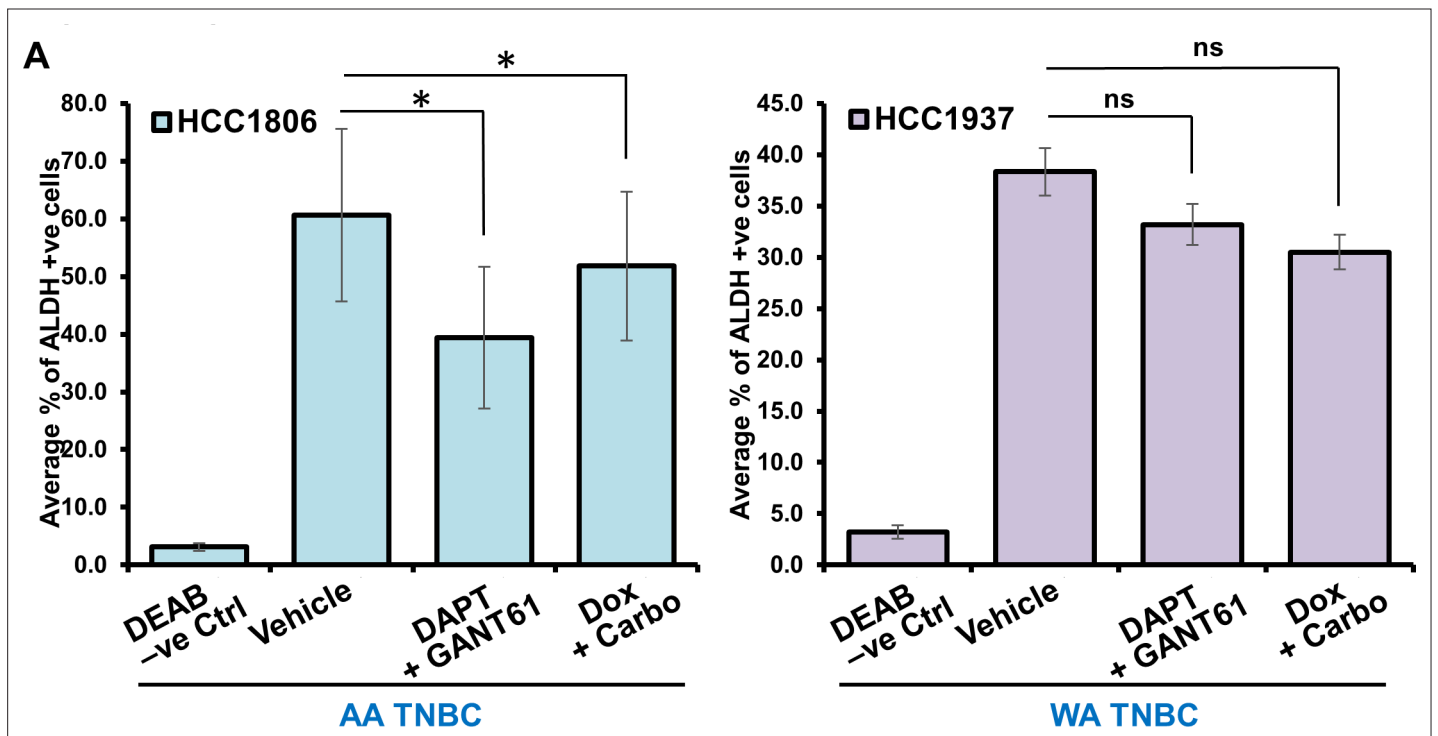
Figure 6 continued on next page

*Figure 6 continued*

stained tumor sections from HCC1806-derived tumors. Scale bar, 100  $\mu\text{m}$ . **(D–H)** Resected tumors from control and treated groups were dissociated and isolated tumor cells were subjected to in vitro functional assays. **(D)** Bar graph shows the migration potential of tumor cells isolated from various treatment groups and control. **(E)** Bar graph shows the number of tumor cells invaded through Matrigel. **(F)** Tumor cell spheroids were formed and allowed to migrate. Representative images of spheroids are shown. Graph shows average distance migrated. Data represents  $n = 3$  independent experiments.  $*p \leq 0.05$ ,  $**p \leq 0.01$ ,  $***p \leq 0.001$ . **(G)** Bar graph shows quantification of solid mammospheres formed from various numbers of tumor cells isolated from various treatment groups and control. Data represents  $n = 3$  independent experiments.  $*p \leq 0.05$ ,  $**p \leq 0.01$ ,  $***p \leq 0.001$ . **(H)** Representative images of mammospheres formed from tumor-dissociated cells. **(I)** Flow cytometry analysis of dissociated tumor cells using CD44 and CD24 staining. **(J)** Representative images of Sox2 and Oct4 stained tumor sections from HCC1806-derived tumors from control and treatment groups. Scale bar, 100  $\mu\text{m}$ .

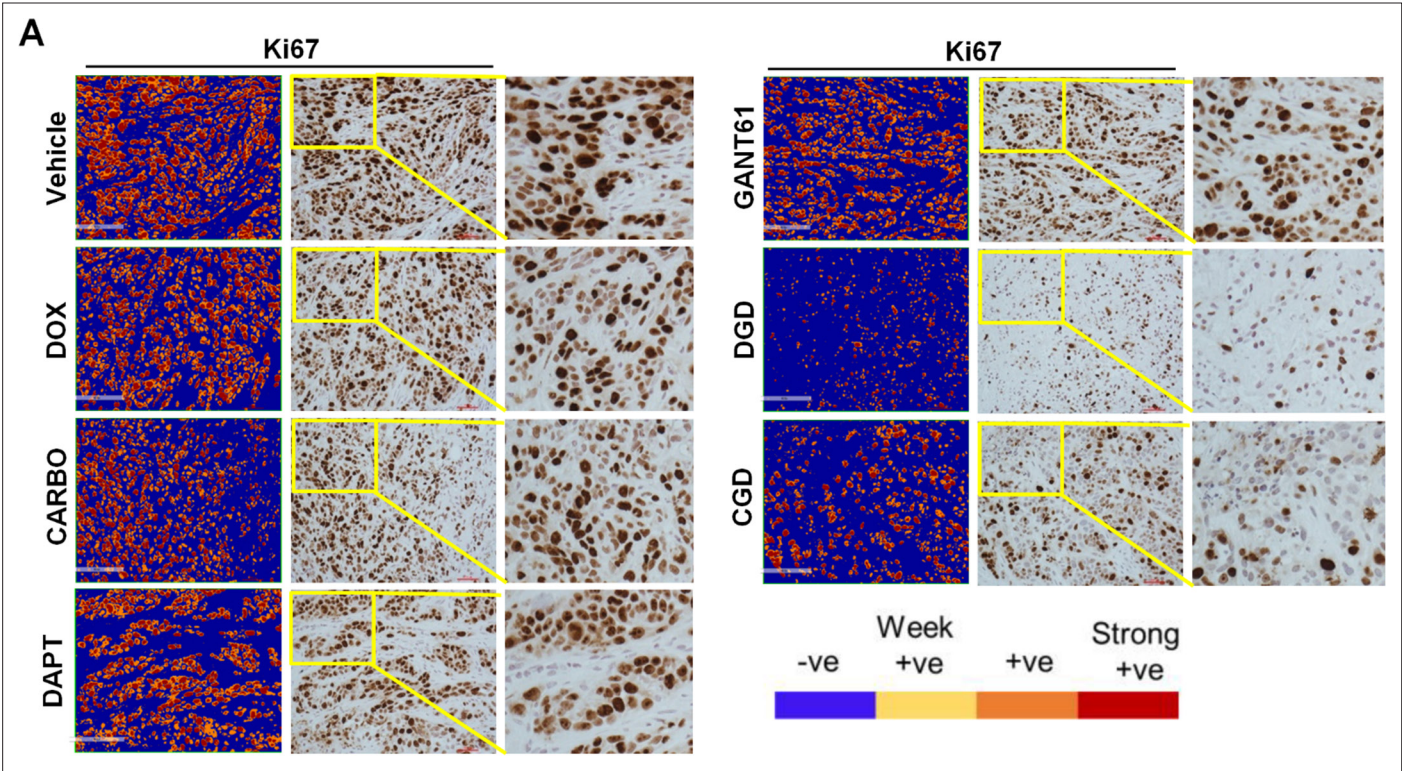


**Figure 6—figure supplement 1.** Effect of GLI inhibitor + Notch inhibitor combination and doxorubicin + carboplatin combination on African American (AA)-triple negative breast cancer (TNBC) and White American (WA)-TNBC cells. Line graphs show tumor progression curves of HCC1806-derived tumors ( $n = 6$ ), HCC1937-derived tumors ( $n = 6$ ), and MDA-MB-231-derived tumors ( $n = 6$ ) treated with vehicle, DAPT (20 mg/kg of body weight, 5 days/week) + GANT61 (50 mg/kg of body weight, twice a week) combination and doxorubicin (2 mg/kg of body weight, once a week) + carboplatin (50 mg/kg of body weight, single dose) combination as indicated. \* $p \leq 0.05$  for DAPT + GANT61 compared to vehicle for HCC1806 tumors. n.s. for DAPT + GANT61 compared to vehicle for HCC1937 and MDA-MB-231 tumors. n.s. not significant.



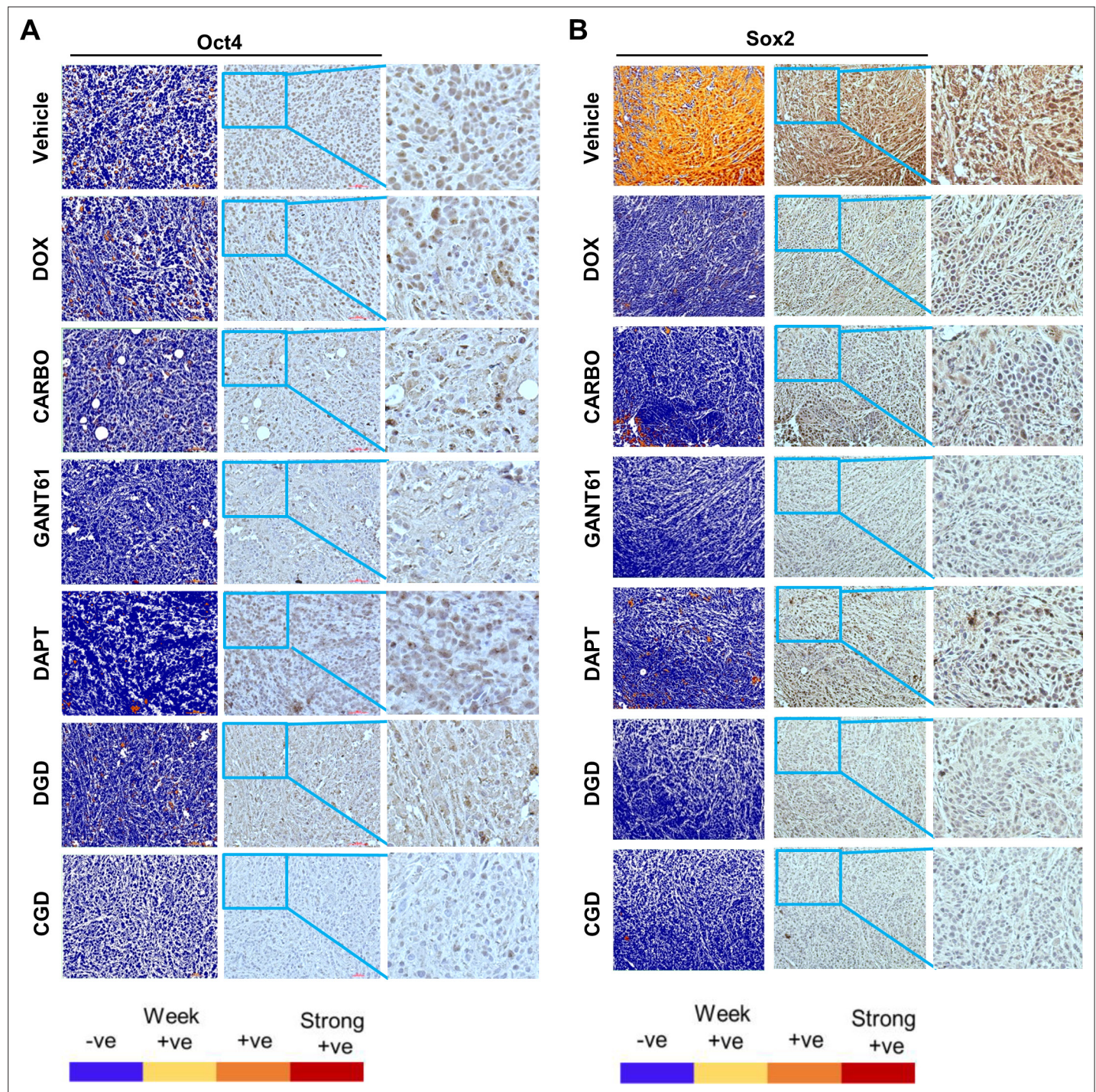
**Figure 6—figure supplement 2.** African American (AA)-triple negative breast cancer (TNBC) tumors treated with a combination of Notch inhibitors and GLI inhibitor exhibit reduced ALDH activity. ALDH activity assay for dissociated tumor cells from HCC1937 and HCC1806 tumors treated with DAPT + GANT61 and doxorubicin + carboplatin combination. Bar graphs show average % of ALDH+ cells (\* $p \leq 0.05$ ). n.s. not significant.





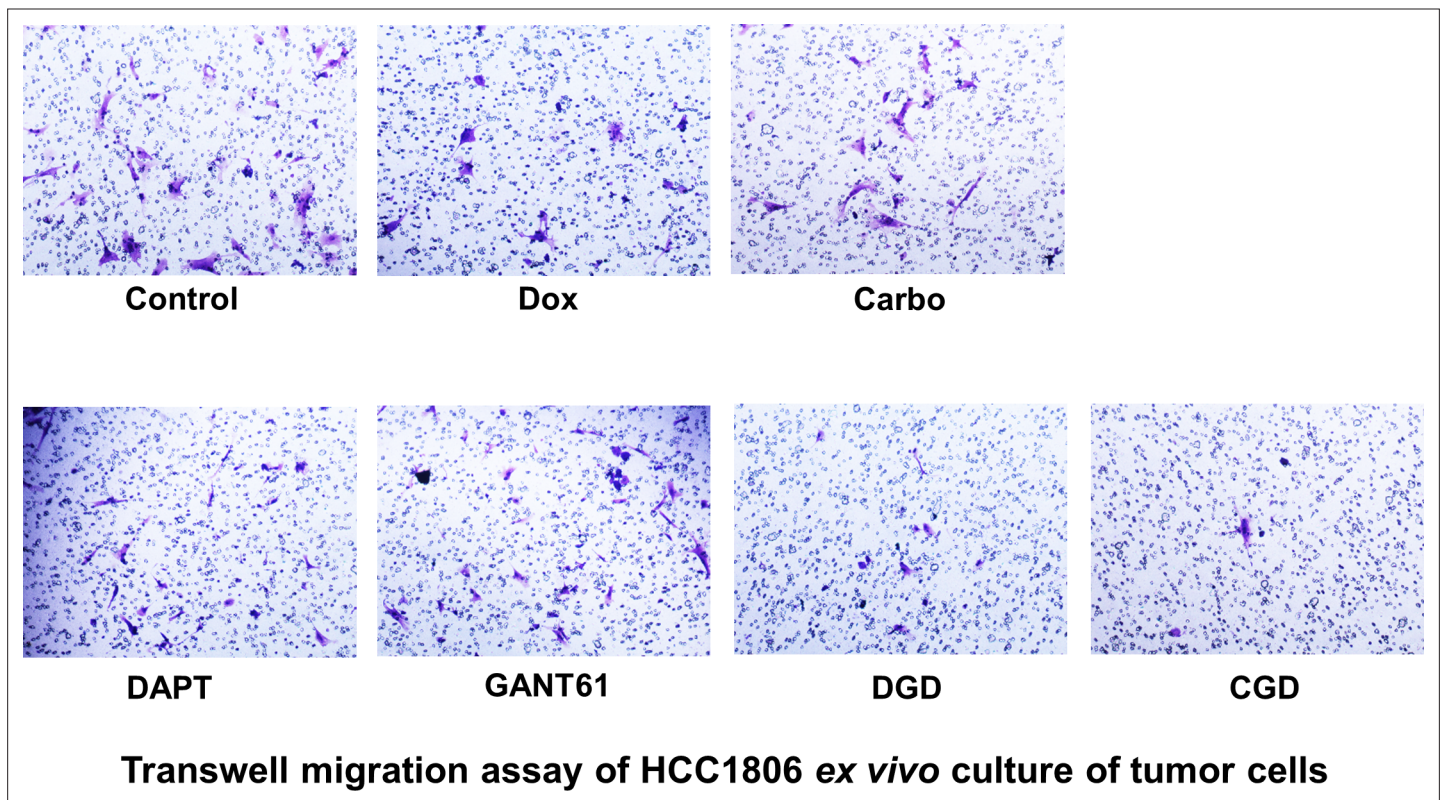
**Figure 6—figure supplement 3.** African American (AA)-triple negative breast cancer (TNBC) tumors treated with a combination of chemotherapy, Notch inhibitor, and GLI1 inhibitor exhibit reduced Ki-67 expression. Representative images of IHC analysis of Ki67 expression in HCC1806-derived tumors developed in mice treated with vehicle, Dox – doxorubicin, Carbo – carboplatin, DAPT, GANT61, DGD – doxorubicin + GANT61 + DAPT or CGD – carboplatin + GANT61 + DAPT. Scale bar, 100  $\mu$ m.



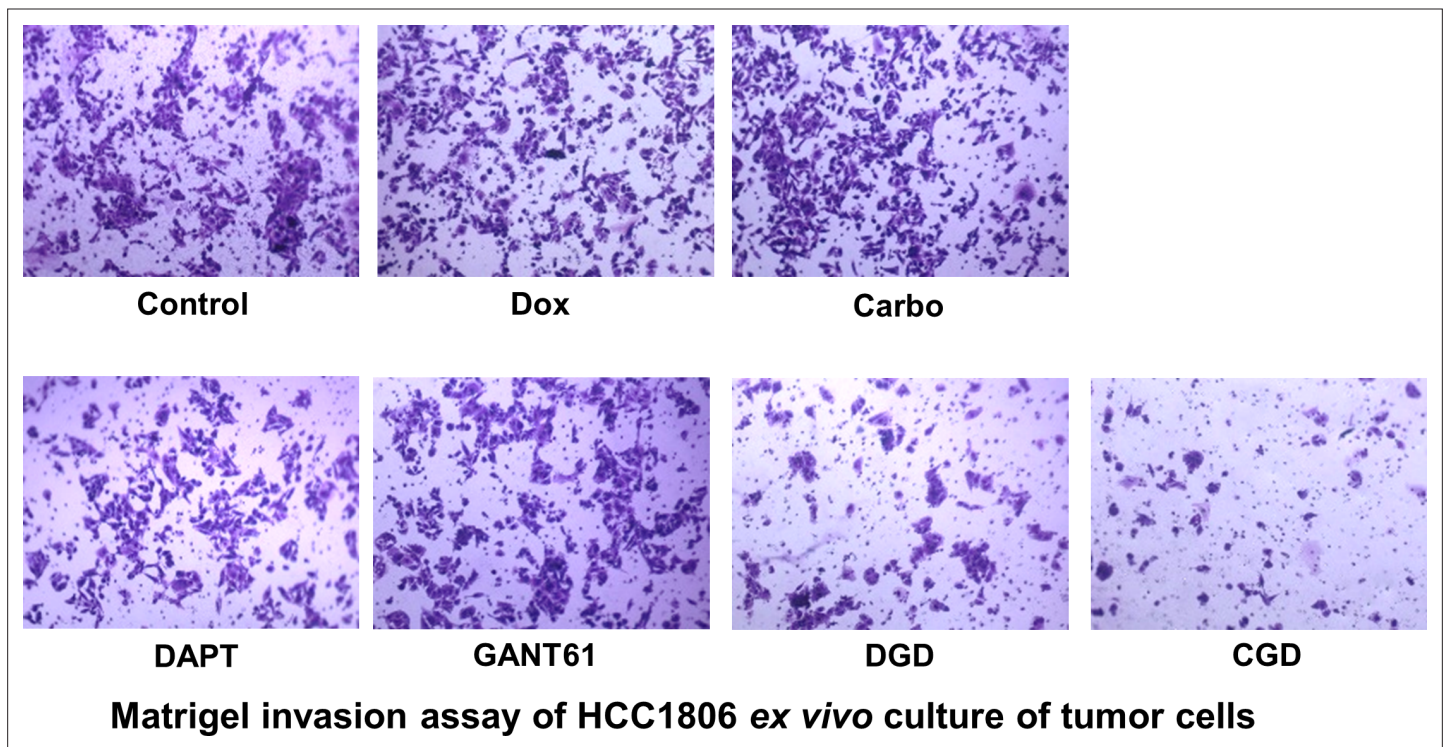


**Figure 6—figure supplement 4.** African American (AA)-triple negative breast cancer (TNBC) tumors treated with a combination of chemotherapy, Notch inhibitor, and GLI1 inhibitor exhibit reduced Oct4 and Sox2 expression. Representative images of IHC analysis of Oct4 and Sox2 expression in HCC1806-derived tumors developed in mice treated with vehicle, Dox – doxorubicin, Carbo – carboplatin, DAPT, GANT61, DGD – doxorubicin + GANT61 + DAPT or CGD – carboplatin + GANT61 + DAPT. Scale bar, 100  $\mu$ m.

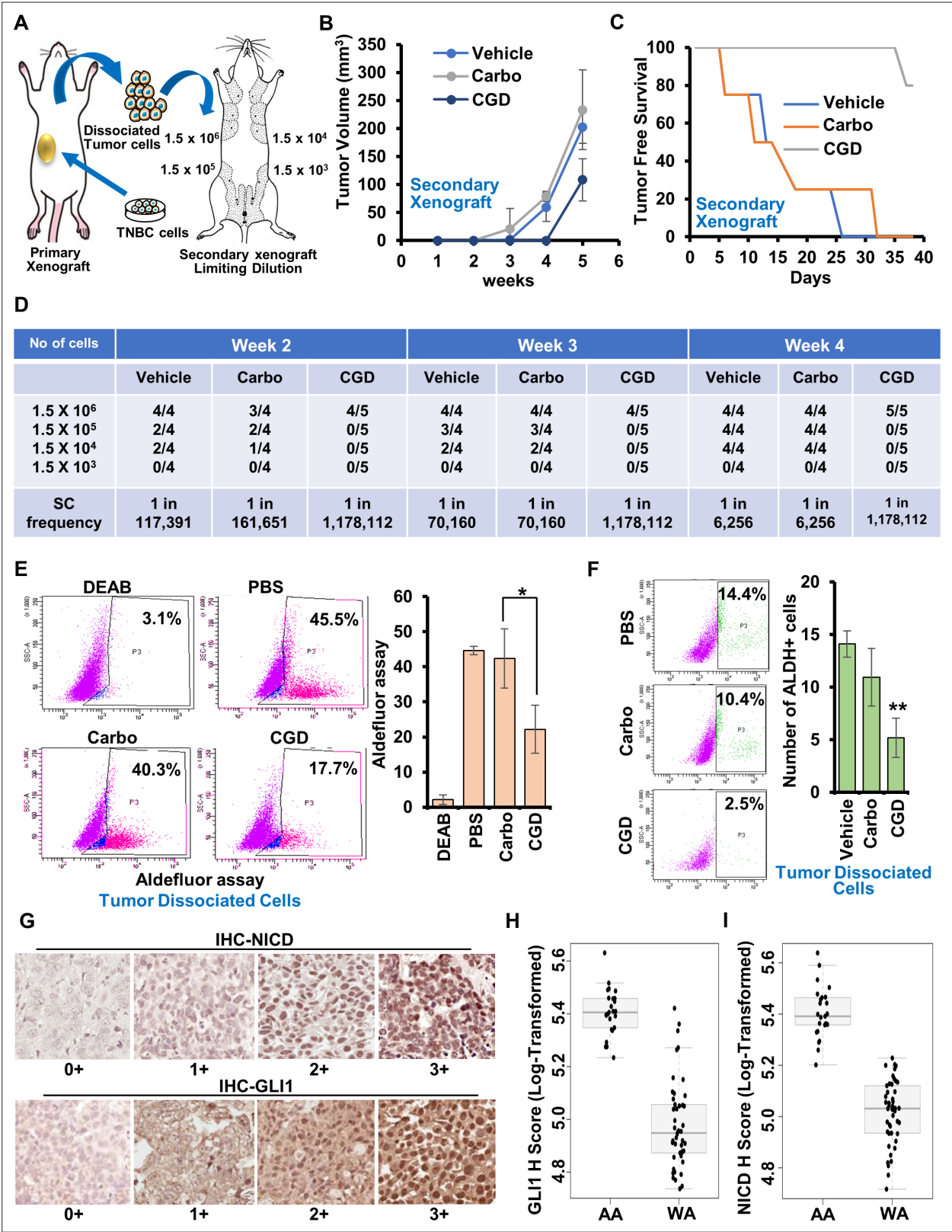




**Figure 6—figure supplement 5.** Combined treatment with chemotherapy, Notch inhibitor, and GLI1 inhibitor reduces migration potential of African American (AA)-triple negative breast cancer (TNBC) tumor-derived cells. Resected tumors from control and treated groups (Dox – doxorubicin, Carbo – carboplatin, DAPT, GANT61, DGD – doxorubicin + GANT61 + DAPT, CGD – carboplatin + GANT61 + DAPT) were dissociated into single cell suspension and isolated tumor cells were subjected to in vitro migration assays. Representative images of cells undergoing transwell migration are shown.



**Figure 6—figure supplement 6.** Combined treatment with chemotherapy, Notch inhibitor, and GLI1 inhibitor reduces invasion potential of African American (AA)-triple negative breast cancer (TNBC) tumor-derived cells. Resected tumors from control and treated groups (Dox – doxorubicin, Carbo – carboplatin, DAPT, GANT61, DGD – doxorubicin + GANT61 + DAPT, CGD – carboplatin + GANT61 + DAPT) were dissociated into single cell suspension and isolated tumor cells were subjected to *in vitro* Matrigel invasion assays. Representative images of cells undergoing Matrigel invasion are shown.



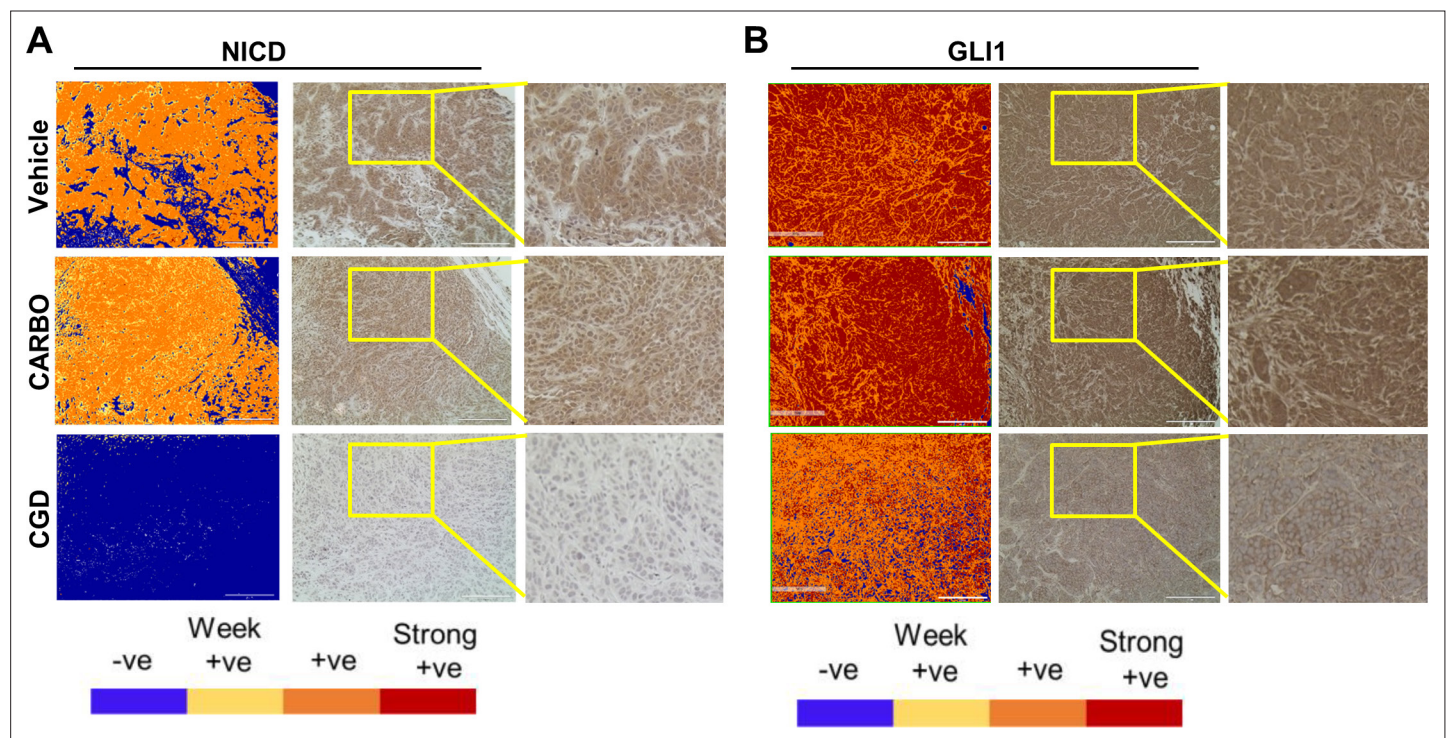
**Figure 7.** Inhibition of Notch and GLI1 enhances the effect of carboplatin in African American (AA)-triple negative breast cancer (TNBC); Notch1 and GLI1 are overexpressed in AA-TNBC tissues in comparison to TNBC tissues from White American (WA) women. **(A)** Schematic outline of the in vivo limiting dilution assay. **(B)** Tumor volume of secondary tumors established with  $1.5 \times 10^6$  tumor-dissociated cells from tumors formed in mammary fat pads of SCID/NOD mice implanted with HCC1806 cells and treated with vehicle, carboplatin (Carbo), or carboplatin + GANT-16 + DAPT (CGD).

Figure 7 continued on next page

*Figure 7 continued*

Secondary xenografts remain untreated. **(C)** Plots show Kaplan–Meier curves (blue – vehicle, orange – carboplatin, gray – CGD) for time to detect tumors in mice bearing secondary tumors. **(D)** Tumor incidence at weeks 2, 3, and 4 of secondary transplants of tumor-dissociated cells from tumors formed with HCC1806 cells and treated with vehicle, carboplatin (Carbo), or carboplatin + GANT-16 + DAPT (CGD) at limiting dilutions. The tumors/numbers of mice/group are shown. The bottom row indicates the estimated breast tumor-initiating/stem cell (SC) frequencies. **(E)** Aldefluor assay using tumor-dissociated cells from secondary tumors formed in in vivo limiting dilution. \* $p \leq 0.05$ . **(F)** Flow cytometry analysis of tumor-dissociated cells from secondary tumors formed in in vivo limiting dilution using ALDH1 staining. \*\* $p \leq 0.01$ . **(G)** Expression of GLI1 and Notch intracellular domain (NICD) in TNBC tissue samples from AA and WA women. Representative images of IHC analysis of NICD and GLI1 expression in TNBC tissue samples from AA and WA women. Images are scored for staining intensity of cells as 0, 1, 2, 3 representing no, mild, moderate, or high staining intensity. **(H)** Graphical representation of GLI1 expression in TNBC tissues from AA women ( $n = 25$ ) and WA women ( $n = 46$ )  $p < 0.001$ . **(I)** Graphical representation of NICD expression in TNBC tissues from AA women ( $n = 25$ ) and WA women ( $n = 46$ )  $p < 0.001$ .





**Figure 7—figure supplement 1.** Reduced expression of Notch intracellular domain (NICD) and GLI1 in African American (AA)-triple negative breast cancer (TNBC) secondary tumors treated with a combination of carboplatin, GANT61, and DAPT. Representative images of IHC analysis of NICD and GLI1 expression in secondary tumors from in vivo limiting dilution assay (groups: vehicle, carboplatin (Carbo), or carboplatin + GANT61 + DAPT [CGD]). Scale bar, 100  $\mu$ m.



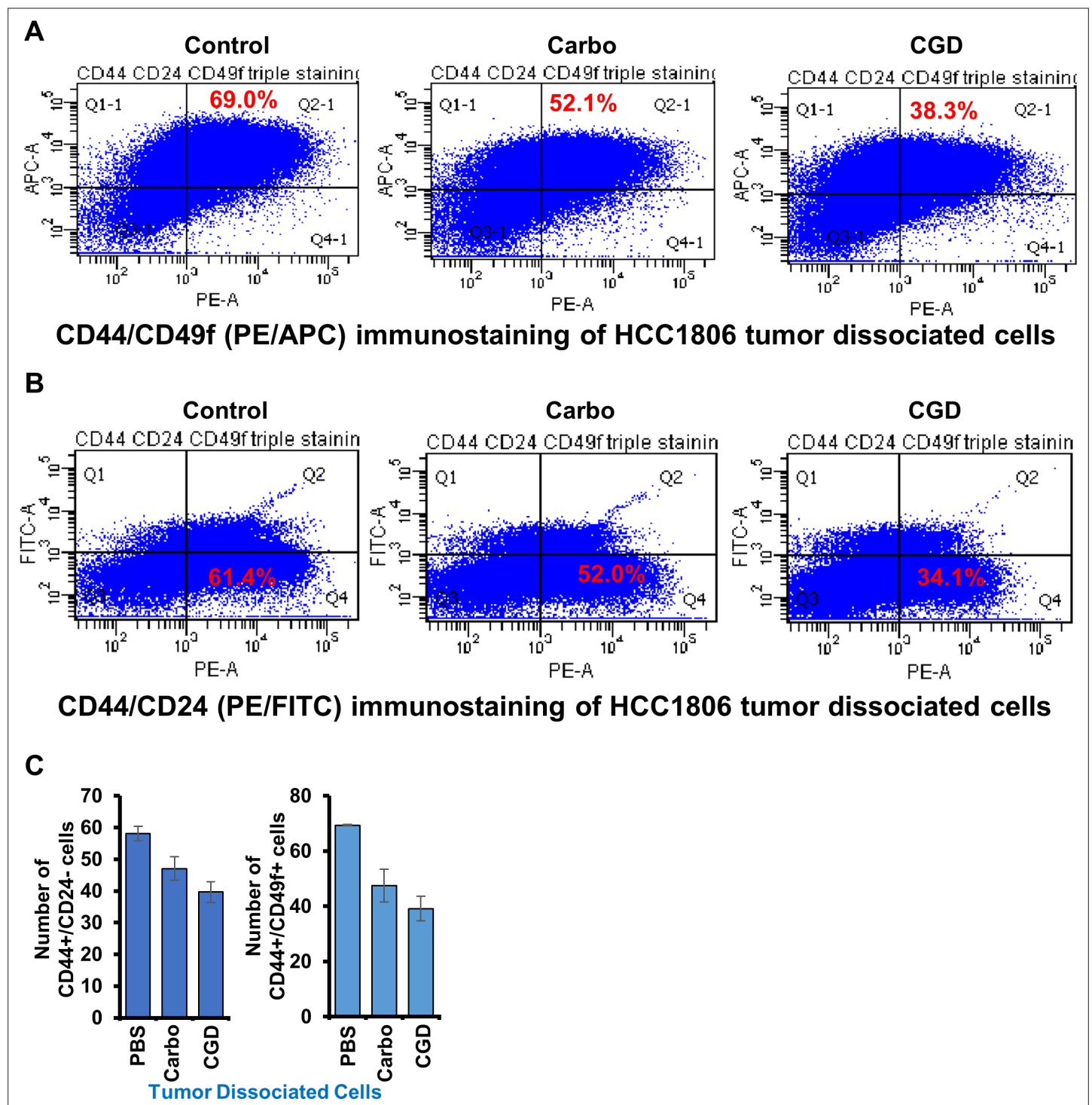


**Figure 7—figure supplement 2.** Inhibition of Notch1 and Gli1 along with carboplatin treatment inhibits stemness African American (AA)-triple negative breast cancer (TNBC) secondary tumors. (A–B) Resected secondary tumors from in vivo limiting dilution assay (groups: vehicle, carboplatin (Carbo), or carboplatin + GANT61 + DAPT [CGD]) were dissociated into single cell suspension and subjected to flow cytometry analysis using CD44 and CD49f staining or CD44 and CD24 staining. (C) Bar graph shows quantitative representation of CD44+/CD49f+ and CD44+/CD24- cells.